Postprint of: Ullah U., Mabrouk I., Kozieł S., A Compact Circularly Polarized Antenna With Directional Pattern for Wearable Off-Body Communications, IEEE Antennas and Wireless Propagation Letters, Vol. 18, iss. 12 (2019), pp. 2523-2527,
DOI: 10.1109/LAWP.2019.2942147

A Compact Circularly Polarized Antenna With Directional Pattern for Wearable Off-Body Communications

Ubaid Ullah, Ismail Ben Mabrouk, and Slawomir Koziel, *Senior Member, IEEE*

***Abstract*—This letter presents a geometrically simple and compact circularly polarized (CP) antenna with unidirectional radiation characteristics for off-body communications. The proposed antenna is based on a microstrip line monopole extension from a coplanar waveguide (CPW) and a protruded stub from one side of the coplanar ground plane along the length of the monopole. The orthogonal components of equal amplitudes required for circular polarization are induced using the vertical stub and the horizontal edge of the coplanar ground plane. To control the radiation of the antenna towards the human body, a flexible, high permittivity laminated substrate is used as a reflector. The topological simplicity of the antenna permits a small number of adjustable variables and therefore a reduced computational cost of the parameter tuning process. The total footprint of the proposed antenna is only $0.23\lambda_0 \times 0.24\lambda_0 = 0.05\lambda_0^2$, at the lowest operating frequency. The antenna is numerically and experimentally characterized in the free-space and on a real human volunteer. The simulated and measured reflection coefficient indicates that the operating range of the antenna extends from 5.16 GHz to 6.13 GHz range with 100-percent bandwidth overlap between the impedance bandwidth and the axial ratio (AR) bandwidth. The peak gain of the antenna is 6.22 dBic with a stable radiation pattern in the +z-direction, high efficiency of 90%, and 0.131W/g SAR. The antenna can be used for Unlicensed National Information Infrastructure (U-NII) worldwide band and ISM 5.8 GHz band.**

***Index Terms*— circularly polarized antenna, compact antennas, wearable antenna, EM-driven design.**

I. Introduction

In recent years, the demand for body-centric wireless communication has been growing at an unprecedented rate. Wearable devices are used in health care, sportsmen monitoring, position navigation, coordination during military operations but also as a fashion accessory [1-3]. These devices have been designed and implemented for different frequency bands such as wireless local area network (WLAN) or wireless body area network (WBAN) [4-6]. Modern body-worn medical devices are generally able to continuously monitor and transmit data related to the patient blood pressure, heart rate, metabolic activity and electrocardiogram (ECG). An antenna, being a crucial component of any wireless communication system, plays an important role in maintaining a stable performance of wearable devices. In any body-worn device, the antenna is in close proximity to the human body which is a large volume of high-permittivity and lossy material, severely affecting the electrical characteristics of the antenna [7-9]. On the other hand, the antenna needs to be lightweight, low profile, small size and should radiate minimum amount of energy towards the human body so that the legal limit of the specific absorption rate (SAR) is not violated [8-11].

Generally, antennas of planar geometries are preferred for wearable applications due to the ease of integration and conformability to the body. There is a number of techniques and materials used for the design of wearable antennas, which include the utilization of textile-based materials as a substrate [12-17] [25]. The disadvantage of textile materials is their low conductivity and fast deterioration of antenna characteristics due to the structural deformation associated with the body movements and changes in the body posture. Also, poor conductivity of the materials results in low efficiency of the antenna. Another disadvantage of using textile-based substrates is in the complexity of integrating and soldering other active/passive circuit components to the communication system [2]. Moreover, the polarization mismatch for linearly polarized (LP) antenna is an important issue. On the other hand, CP antennas has the advantage of reduced multipath losses, absorption losses and signal attenuation. The presence of a human body and its movements increases the polarization loss factor and, consequently, degrades the quality of communication and accuracy of data transmission. To overcome the issue and to mitigate polarization mismatch losses, CP antennas were proposed but most of the available designs were targetting the 2.4 GHz band [18-22]. From the point of view of ensuring higher data rates, improved channel capacity, and compact size of the antenna for body-centric applications, the 5 GHz band seems to be more suitable. Unfortunately, the research on wearable antennas for the 5 GHz band has been limited to date.

In this letter, a geometrically simple, low profile, and compact size antenna has been designed for 5 GHz band wearable applications. The proposed antenna topology is based on a coplanar waveguide (CPW)-fed microstrip line monopole and a vertical stub extension from one of the coplanar ground planes. Circular polarization is achieved by inducing orthogonal components of equal amplitudes by a vertically protruded stub

Manuscript submitted on June 30, 2019. This work was supported in part by the ADEK Award for Research Excellence (AARE) 2018. the Icelandic Centre for Research (RANNIS) Grant 174114051, and by the National Science Centre of Poland Grant 2017/27/B/ST7/00563.

U.Ullah and Ismail Mabrouk are with Networks and Communication Engineering department, Al Ain university of Science and Technology, P.O.Box (112612), Abu Dhabi, UAE. (ubaid.ullah@aau.ac.ae, ismail.mabrouk@aau.ac.ae). S. Koziel is with Engineering Optimization and Modeling Center of Reykjavik University, Reykjavik, Iceland and also with the Faculty of Electronics, Telecommunications and Informatics, Gdansk University of Technology, 80-233 Gdansk, Poland (e-mail: koziel@ru.is).

This article has been accepted for publication in a future issue of this journal, but has not been fully edited. Content may change prior to final publication. Citation information: DOI 10.1109/LAWP.2019.2942147, IEEE Antennas and Wireless Propagation Letters

from the right-side coplanar ground plane and the horizontal edge of the left-side ground plane. To ensure unidirectional radiation, essential for off-body wearable applications, and to reduce the loading effects of the human body, a flat reflector of a high permittivity laminated substrate is placed a quarter wavelength away from the antenna. Due to topological simplicity, the antenna is described using only a few parameters, which facilitates its EM-driven design closure. The optimized design is prototyped and characterized in free space and on-body and the measured results are compared with the simulation. The total antenna footprint is only $0.05\,\lambda_o^2$, which can be easily fit to any wearable device or even button of the cloths. A 100-percent bandwidth overlap between impedance bandwidth and AR bandwidth is achieved with the peak gain of the antenna is 6.22 dBi and stable radiation pattern characteristics. This paper contributes to: (i) design of a unidirectional CP antenna covering U-NII worldwide band and ISM 5.8 GHz band; (ii) reduced loading effects of the human body owing to the unidirectional topology and high permittivity substrate used as a reflector; (iii) a simple low profile structure, compact size (178mm^2), high efficiency and low SAR.

II. Antenna Design Configuration And Analysis

A. Antenna Design

A configuration of the proposed antenna design is shown in Fig. 1. The antenna topology is printed on the front of a single-layer laminated Rogers substrate RO4003C with permittivity ε_r = 3.38, tangent loss tanδ = 0.0027, thickness h = 0.813 mm and external dimension $L_s \times W_s$. The antenna is fed through a 50-Ohm coplanar waveguide with a quarter wavelength microstrip line monopole extension of the length L_m and width W_m = 1.75 mm. The gap g between the microstrip line and the coplanar ground planes is fixed at 0.6325 mm. A stub of the length L_1 is protruded from one side of the coplanar ground plane along the length of the microstrip line. The orthogonal electric field components of equal amplitudes are induced in the antenna by appropriate sizing of the width of the coplanar ground plane in the x-direction and the stub in the y-direction. As the antenna is designed for off-body wearable applications, a flat reflection is added behind the antenna to direct all the radiated power away from the body. To reduce the loading effects on a human body, a high permittivity substrate RO3010 (ε_r = 10.2, tanδ = 0.0027, thickness h = 0.635) is used to implement the reflector. For maximum directivity in the off-body direction, the reflector is positioned at a distance H = ~13 mm which is a quarter wavelength corresponding to the center operating frequency of the antenna.

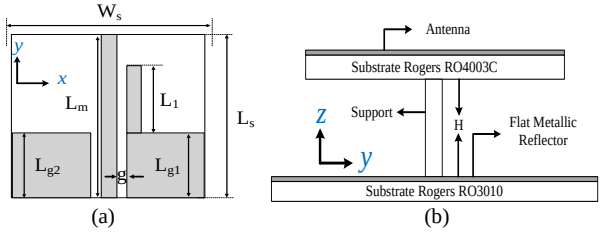

Fig. 1. Geometry of the proposed CP antenna (All values in mm): (a) top view (b) side view. L_1= 6.39, L_{g1}=5.39, L_{g2}=6.1, L_m=13.74, L_s=13.77, and W_s= 12.99.

B. Antenna Development Stages

The proposed antenna has been developed in three stages as depicted in Fig. 2. In the first stage, a simple CPW fed microstrip line monopole antenna is designed. The impedance matching characteristic (cf. Fig. 3(a)) shows a resonance near 5.4 GHz, which due to the quarter wavelength monopole; the antenna is purely LP. In the second stage, a stub is protruded from the right-side ground plane which induces an additional electric field component along the y-direction and generates CP radiation as depicted in Fig. 3(b). In the final stage, to further improve the impedance matching and axial ratio, the symmetry of the CPW is slightly broken and all the adjustable variables are optimized.

C. Antenna CP Mechanism

The circular polarization mechanism of the antenna is illustrated in Fig. 4 with the phase progression at different time instants. The orthogonal electric field components E_x and E_y are explained with the help of the surface current distribution at the CP center frequency.

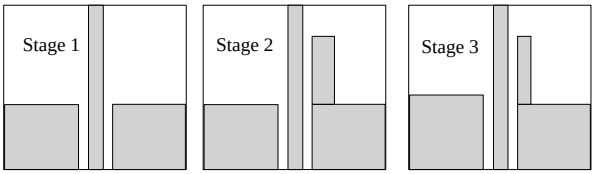

Fig. 2. Antenna evolution stages.

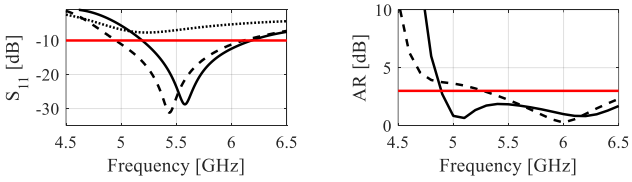

Fig. 3. Antenna impedance matching and AR response through the development stages: Stage 1 (….), Stage 2 (----), and Stage 3 (—): (a) S_{11} (b) AR.

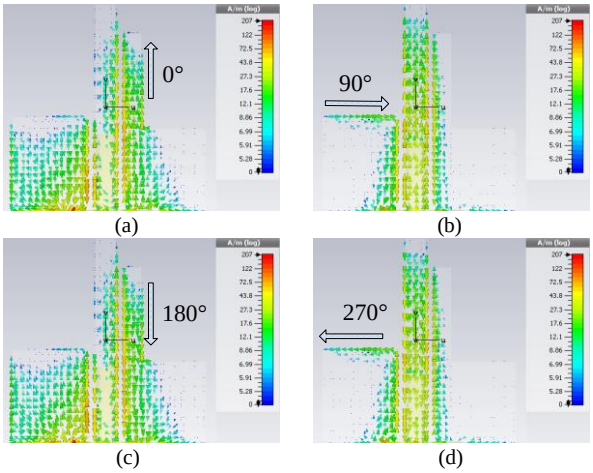

Fig. 4. Circular polarization mechanism of the proposed antenna: (a) 0-degree (b) 90-degree (c) 180-degree (d) 270-degree.

This article has been accepted for publication in a future issue of this journal, but has not been fully edited. Content may change prior to final publication. Citation information: DOI 10.1109/LAWP.2019.2942147, IEEE Antennas and Wireless Propagation Letters

As shown in Fig. 4(a), at zero degrees, the dominant field components are oriented along the *y*-direction at the periphery of the extended stub from the right-side ground plane. At 90 degrees (Fig. 4(b)), the dominant field is concentrated at the edge of the ground plane along its width in the *x*-direction. Similarly, at 180 degrees, the fields are seen to be changing their orientation from the *x*-direction to the *y*-direction, and at 270 degrees the pattern of rotation repeats itself. As the electric field vector is rotating in the clockwise direction, the sense of polarization of the antenna is right-hand CP (RHCP).

D. Parametric Analysis

The effects of the key antenna parameters, L_1, W_1, L_{g1} and L_{g2}, on the reflection coefficient and AR have been examined in Fig. 5. It can be observed that increasing L_1 lowers the resonant frequency (from 5.16 GHz to 5.0 GHz for the considered range) and the AR is detuned and shifted upwards. When the value of L_1 is decreased, the impedance bandwidth of the antenna is affected and the AR is shifted upwards. The reflection coefficient is not very sensitive W_1 but it slightly affects the AR at the lower operating frequency. L_{g1} has a similar effect as L_1 on both the impedance bandwidth and AR. This is because both parameters effectively change the length of the right-side coplanar ground plane. Moreover, the parameter L_{g2} plays an important role in tuning the resonant frequency as it can be seen in Fig. 5. Varying L_{g2} permits tuning the operating frequency. On the other hand, L_{g2} has an almost negligible effect on the AR, which is because the orthogonal component of CP is excited along the width of the left-side ground plane (See Fig. 4.).

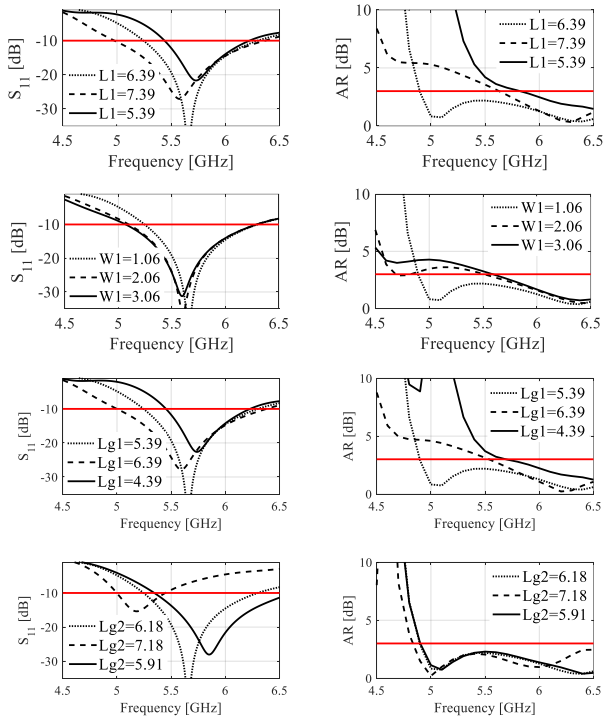

Fig. 5. Parametric analysis of the antenna in terms of $|S_{11}|$ and AR.

III. EXPERIMENTAL VALIDATION

A. Return Loss and Axial Ratio analysis

The antenna prototype has been fabricated and characterized in the free space and on-body in the anechoic chamber of Reykjavik University, Iceland. The prototype of the antenna, on-body characterization setup (arm and chest) is shown in Fig. 6. The impedance matching responses are depicted in Fig. 7 (a). The free space impedance bandwidth response shows that the antenna is operating in the range from 5.16 GHz to 6.2 GHz. A similar response is observed when the antenna is measured on the arm and the chest of a human volunteer (22 years of age, weight 83 kg, height 180 cm). The antenna is mounted on the arm and the chest on the top of the volunteer cloths. The separation between the antenna and the human body is roughly 3 mm which is the same as that used for numerical analysis of the antenna. The impedance matching remains well below -22 dB for all cases with a slight degradation and upward shift in the resonance frequency as compared to simulation.

Figure 7(b) shows the axial ratio characteristics for the same setups. Again, there is a small variation in the AR at the upper operating frequency of the antenna, but the 3 dB reference criteria are not violated for all conditions. This indicates suitability of the proposed antenna for wearable applications. At this point, it is important to mention that by using a high permittivity flexible substrate as a reflector, the loading effect of the human body is visibly reduced and the impedance bandwidth and AR remain close to those at the free space.

B. Realized Gain and Efficiency Analysis

The realized gain characterization in the free-space and on-body are depicted in Fig. 8. The simulated and measured responses in the free space show a stable gain response in the entire operating bandwidth with the peak gain of 6.22 dBic. A gain drop of roughly 1 dB can be observed at the lower end of the operating frequency when the antenna is mounted on the chest of the volunteer. The measured on-arm gain exhibits a slight drop in the upper part of the frequency spectrum. Figure 9 shows the simulated and measured total efficiency of the antenna in the free-space and on the body.

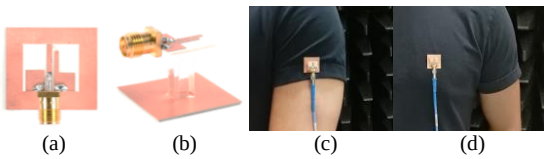

Fig. 6. Antenna prototype and characterization: (a) Front view (b) perspective view (c) On-arm (d) On-chest.

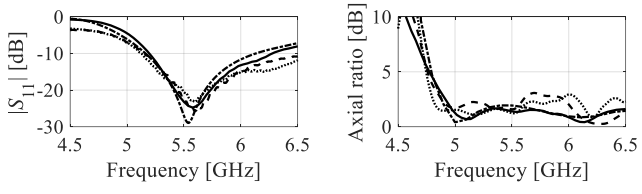

Fig. 7. Antenna reflection coefficient and AR response: Measured (——), measured on chest (----), measured on arm (….), simulated (- · -). (a) $|S_{11}|$ (b) AR.

This article has been accepted for publication in a future issue of this journal, but has not been fully edited. Content may change prior to final publication. Citation information: DOI 10.1109/LAWP.2019.2942147, IEEE Antennas and Wireless Propagation Letters

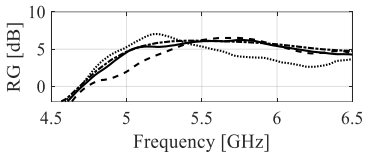

Fig. 8. Antenna realized gain: measured (——), measured on chest (----), measured on arm (….), simulated (- · - · -), simulated on body (-o-).

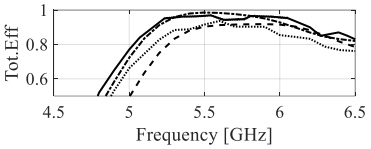

Fig. 9. Antenna Efficiency: measured (——), simulated on chest (----), simulated on arm (….),simulated (- · - · -).

The simulated and measured efficiency of the antenna in the free-space is 99% and 97%, respectively. When the antenna is mounted on arm the efficiency drops to 80% near the lower edge of the operating frequency and remains around 90% at the center and the upper cut-off frequency. A similar behavior is observed for the case when the antenna is tested on the chest. At the lower frequency, the efficiency drops to roughly 70% but it is maintained at approximately 90% within the overall operating bandwidth of the antenna. Table I show a comparison of major performance figures for the proposed design and the recent state-of-the-art antennas from the literature.

C. Radiation Pattern and Specific Absorption Rate Analysis

The radiation pattern of the proposed antenna in the *xz*- and *yz*-plane is shown in Figs. 10. A stable unidirectional RHCP radiation pattern is realized in the +*z*-direction with a close agreement between the simulated and the measured data.

Specific absorption rate (SAR) is an important factor for wearable antennas. It is the measurement of the energy absorbed by the per unit mass of the human tissue. SAR depends on the conductivity (σ), electric field intensity (E) and mass density (ρ), according to the formula $SAR = E^2/\rho$. The proposed antenna is analyzed for SAR on a human phantom as shown in Fig. 11. The SAR is evaluated for 1 g and 10 g of body tissue and the maximum SAR value recorded was 0.182 W/kg and 0.106 W/kg on arm, while 0.131 W/kg and 0.097 W/kg on the chest respectively. All the SAR values are within the safety limits of 1.6W/kg defined by the United States.

IV. Conclusion

In this letter, a compact and high efficiency CP antenna has been proposed for body-centric applications. The antenna employs a CPW-fed radiator and a high permittivity flexible substrate reflector to ensure off-body unidirectional ration pattern. The simple topology of the antenna requires only a few adjustable parameters which enables fast EM-driven optimization. The multi-layer design, although not as convenient as single-layer implementations, effectively alleviates the negative effects of the human body proximity on antenna performance. The antenna has been tested in the free space and on the body (arm and chest) through simulation, and, subsequently, validated experimentally.

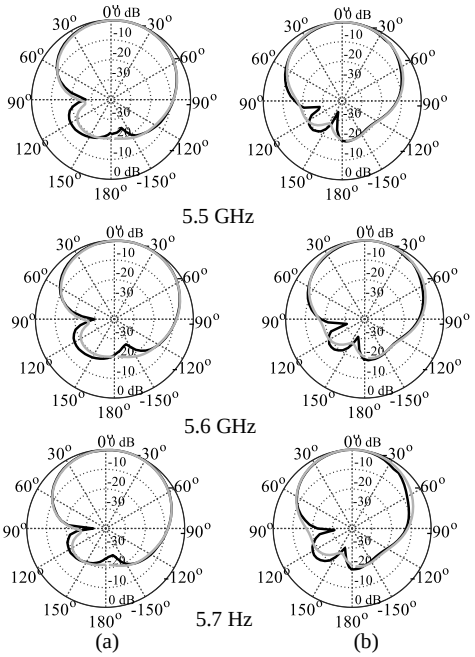

Fig. 10. Simulated (gray) and measured (black) radiation pattern of the proposed antenna in (a) the *xz*-plane, and (b) the *yz*-plane. RHCP and LHCP showed using solid and dashed lines, respectively.

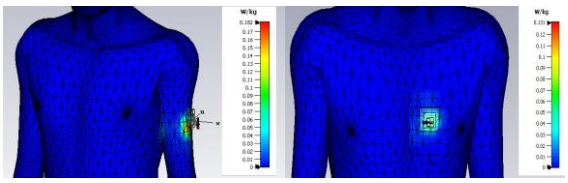

Fig. 11. SAR analysis of the proposed antenna. arm (left) chest (right).

TABLE I Comparison with State-of-The-Art CP Antennas

Ref.	Frequency (GHz)	%AR	%BW	Size [λ_o^2]	Efficiency (%)	Gain (dBi)
[19]	5.47	7	14	---	--	3.5
[20]	3.75	12.5	12.5	0.122	80	5.2
[21]	2.4	2.72	15.9	0.17	79	5.2
[22]	5.57	--	5.4	0.087	48	4.85
[23]	2.4	--	7.75	0.10	75	2.06
[24]	2.45	0.7	0.736	0.46	70	5.1
Proposed	5.16	18.3	18.3	0.05	90	6.2

The high permittivity substrate used for the reflector directs all the radiated energy in the off-body direction and also reduces the loading effects of the human body on the antenna electrical characteristics. The antenna maintains an excellent impedance matching (>-22 dB), and AR (>3 dB) in both free space and on-body scenarios. The peak gain of the antenna is 6.22 dBic, efficiency of 90% when worn on the body, and the SAR values of 0.182 W/kg (arm) and 0.131 W/kg (chest). The antenna is suitable for wearable applications in U-NII band and ISM 5.8 GHz band.

Acknowledgment

The authors would like to thank Dassault Systemes, France, for making CST Microwave Studio available.

This article has been accepted for publication in a future issue of this journal, but has not been fully edited. Content may change prior to final publication. Citation information: DOI 10.1109/LAWP.2019.2942147, IEEE Antennas and Wireless Propagation Letters

REFERENCES

[1] N. Haga, K. Saito, M. Takahashi, and K. Ito, "Characteristics of cavity slot antenna for body-area networks," *IEEE Trans. Antennas Propag.*, vol. 57, no. 4, pp. 837–843, Apr. 2009.

[2] P.S. Hall and Y. Hao, *Antennas and propagation for body-centric wireless communications*. Artech House, Norwood, MA, USA, 2012.

[3] Z. Hamouda, J.-L. Wojkiewicz, A. A. Pud, L. Kone, S. Bergheul, and T. Lasri, "Flexible UWB organic antenna for wearable technologies application," *IET Microwawes Antennas Propag.*, vol. 12, no. 2, pp. 160–166, Jul. 2018.

[4] H.-B. Li, K.-I. Takizawa, B. Zhen, and R. Kohno, "Body area network and its standardization at IEEE 802.15. MBAN," *in Proc. 16th IST Mobile Wireless Commun. Summit*, Jul. 2007, pp. 1–5.

[5] G. Fang, E. Dutkiewicz, M. A. Huq, R. Vesilo, and Y. Yang, "Medical body area networks: Opportunities, challenges and practices," *in Proc. Commun. Inf. Technol. Int. Symp.*, Oct. 2011, pp. 562–567.

[6] S. Yan, P. J. Soh, and G. A. E. Vandenbosch, "Wearable dual-band magneto-electric dipole antenna for WBAN/WLAN applications," *IEEE Trans. Antennas Propag.*, vol. 63, no. 9, pp. 4165–4169, Sep. 2015.

[7] H. Mazar, "Human radio frequency exposure limits: An update of reference levels in Europe, USA, Canada, China, Japan, and Korea," in *Proc. Int. Symp. Electromagn. Compat.*, pp. 467–473, 2016.

[8] C. T. Islam, M. R. I. Faruque, and N. Misran, "Reduction of specific absorption rate (SAR) in the human head with ferrite material and meta-material," *Prog. Electromagn. Res.*, vol. 9, pp. 47–58, Jan. 2009.

[9] H. Cao, V. Leung, C. Chow, and H. Chan, "Enabling technologies for wireless body area networks: A survey and outlook," *IEEE Commun. Mag.*, vol. 47, no. 12, pp. 84–93, Dec. 2009.

[10] A.Y.I. Ashyap *et al.*, "Compact and low-profille textile EBG-based antenna for wearable medical applications," *IEEE Antennas Wireless Propag. Lett.*, vol. 16, pp. 2550–2553, 2017.

[11] P.J. Soh, G. A. E. Vandenbosch, S. L. Ooi, and N. H. M. Rais, "Design of a broadband all-textile slotted PIFA," *IEEE Trans. Antennas Propag.*, vol. 60, no. 1, pp. 379–384, Jan. 2012.

[12] K. Kamardin, M. K. A. Rahim, P. S. Hall, N. A. Samsuri, T. A. Latef, and M. H. Ullah, "Planar textile antennas with artificial magnetic conductor for body-centric communications," *Appl. Phys. A, Mater. Sci. Process.*, vol. 122, no. 4, p. 363, 2016.

[13] S. Zhu and R. Langley, "Dual-band wearable textile antenna on an EBG substrate," *IEEE Trans. Antennas Propag.*, vol. 57, no. 4, pp. 926–935, Apr. 2009.

[14] S. Agneessens and H. Rogier, "Compact half diamond dual-band textile HMSIW on-body antenna," *IEEE Trans. Antennas Propag.*, vol. 62, no. 5, pp. 2374–2381, May 2014.

[15] S. Agneessens, S. Lemey, T. Vervust, and H. Rogier, "Wearable, small, and robust: The circular quarter-mode textile antenna," *IEEE Antennas Wireless Propag. Lett.*, vol. 14, pp. 1482–1485, 2015.

[16] R. K. Shaw, B. R. Long, D. H. Werner, and A. Gavrin, "The characterization of conductive textile materials intended for radio frequency applications," *IEEE Antennas Propag. Mag.*, vol. 49, no. 3, pp. 28–40, Jun. 2007.

[17] M. Wang et al., "Investigation of SAR reduction using flexible antenna with metamaterial structure in wireless body area network," *IEEE Trans. Antennas Propag.*, vol. 66, no. 6, pp. 3076–3086, Jun. 2018.

[18] M. A. B. Abbasi, S. S. Nikolaou, M. A. Antoniades, M. N. Stevanovi¢, and P. Vryonides, "Compact EBG-backed planar monopole for BAN wearable applications," *IEEE Trans. Antennas Propag.*, vol. 65, no. 2, pp. 453–463, Feb. 2017.

[19] X. Hu, S. Yan, and G. A. E. Vandenbosch, "Compact circularly polarized wearable button antenna with broadside pattern for U-NII worldwide band applications," *IEEE Trans. Antennas Propag.*, vol. 67, no. 2, pp. 1341-1345, Feb. 2019.

[20] Z. H. Jiang and D. H. Werner, "A compact, wideband circularly polarized co-designed filtering antenna and its application for wearable devices with low SAR," *IEEE Trans. Ant. Propag.*, vol. 63, no. 9, pp. 3808-3818, Sept. 2015.

[21] Z. H. Jiang, Z. Cui, T. Yue, Y. Zhu, and D. H. Werner, "Compact, highly efficient, and fully flexible circularly polarized antenna enabled by silver nanowires for wireless body-area networks," *IEEE Trans. Biomedical Circuits Syst.*, vol. 11, no. 4, pp. 920-932, Aug. 2017.

[22] Y. J. Li, Z. Y. Lu, and L. S. Yang, "CPW-fed slot antenna for medical wearable applications," *IEEE Access*, vol. 7, pp. 42107-42112, 2019.

[23] A. Arif, M. Zubair, M. Ali, M. U. Khan, and M. Q. Mehmood, "A compact, low-profile fractal antenna for wearable on-body WBAN applications," *IEEE Ant. Wireless Propag. Lett.*, vol. 18, no. 5, pp. 981-985, May 2019.

[24] K. N. Paracha, S.K.A. Rahim, P.J. Soh, M.R. Kamarudin, K.-G. Tan, Y.C. Lo, and M.T. Islam, "A low profile, dual-band, dual polarized antenna for indoor/outdoor wearable application," *IEEE Access*, vol. 7, pp. 33277-33288, 2019.

[25] H. Xiaomu, S. Yan and G. A. E. Vandenbosch, "Wearable button antenna for dual-band WLAN applications with combined on and off-body radiation patterns," IEEE Transactions on Antennas and Propagation, vol. 65, no. 3, pp. 1384-1387, March 2017.